J|A|C|S
ARTICLES
Published on Web 03/30/2006

Role of Interstitial Voids in Oxides on Formation and Stabilization of Reactive Radicals: Interstitial HO_2 Radicals in F_2-Laser-Irradiated Amorphous SiO_2

Koichi Kajihara,* Masahiro Hirano, Linards Skuja,† and Hideo Hosono‡

Contribution from the Transparent Electro-Active Materials Project, ERATO-SORST, Japan Science and Technology Agency, Frontier Collaborative Research Center, Mail Box S2-13, Tokyo Institute of Technology, 4259 Nagatsuta, Midori-ku, Yokohama 226-8503, Japan

Received October 20, 2005; E-mail: kaji2@lucid.msl.titech.ac.jp

Abstract: A procedure to produce stable hydroperoxy radicals ($HO_2^\bullet$) in bulk amorphous SiO_2 (*a*-SiO_2) has been developed. Oxygen molecules incorporated in the interstitial voids in *a*-SiO_2 react with mobile hydrogen atoms (H^0) generated by the photolysis of silanol (SiOH) groups with F_2-laser light ($\lambda = 157$ nm, $h\nu = 7.9$ eV), resulting in the efficient creation of interstitial $HO_2^\bullet$. The high yield of $HO_2^\bullet$ suggests that the collisions of the reaction intermediate with the void wall play an important role in dissipating the excess energy of the intermediate instead of the triple collision observed in the gas phase reaction. The resultant $HO_2^\bullet$ is thermally stable up to 100 °C.

1. Introduction

Reactive oxygen species such as $O^{\bullet-}$, $O_2^{\bullet-}$ (superoxide ion radical), and $O_3^{\bullet-}$ (ozonide ion radical) are important oxidants in the catalytic oxidation of various organic compounds ($^\bullet$ denotes an unpaired electron).[1,2] Their conjugate acids, $HO^\bullet$ (hydroxyl radical), $HO_2^\bullet$ (hydroperoxy radical), and $HO_3^\bullet$ (hydrogen trioxide radical), also act as key intermediates in reactions in acidic solutions or protonic solvents.[3] In actual catalytic reactions, their formation and reactivity are controlled by various catalysts such as metals, metal oxides, zeolites, metal complexes, and their hybrids. Among these, catalytic activity of amorphous SiO_2 (*a*-SiO_2), which is often regarded as inert, has attracted particular interest due to its thermal and chemical stabilities.[4−8] It is considered that the main origin of the catalytic activity of *a*-SiO_2 is nano- and mesopores, which are formed intentionally and are abundantly present in mesoporous silicas and silica gels.[4−6] However, besides these "extrinsic" pores, *a*-SiO_2 contains a lot of "intrinsic" interstitial voids in the Si−O−Si bond network because of its low density (2.2 g cm^{-3}) in comparison to the related crystalline form of SiO_2 (α-quartz, 2.62 g cm^{-3}) and other light metal oxides of analogous formular weight, such as MgO (3.6 g cm^{-3}) and Al_2O_3 (3.97 g cm^{-3}).

The interstitial voids in *a*-SiO_2 often encapsulate small molecules and radical fragments. For example, the hydrogen atom (H^0), which is one of the most reactive radicals, is immobilized in *a*-SiO_2 below ∼100 K.[9−13] Various molecular radicals such as $HCO^\bullet$,[14] $NO_2^\bullet$,[15] and $ClO_x^\bullet$ ($x = 0, 2, 3$)[16,17] have been formed in *a*-SiO_2 exposed to energetic radiation, such as X-rays, γ-rays, or ultraviolet laser light. Such small chemical species can migrate through the interstitial voids in *a*-SiO_2: hydrogen molecules (H_2) diffuse rapidly even at room temperature (average diffusion length ∼10−100 nm in 1 s).[18] Thus, interstitial voids having entrances to the outer surfaces may be accessible for small reactive species to influence reactions catalyzed by *a*-SiO_2.

In this study, we report a novel process for the formation of interstitial $HO_2^\bullet$ in *a*-SiO_2, which contains both interstitial oxygen molecules (O_2) and silanol (SiOH) groups. Bulk *a*-SiO_2 was used to selectively observe reactions among interstitial

† Current address: Institute of Solid State Physics, University of Latvia, Kengaraga iela 8, LV1063 Riga, Latvia.
‡ Current address: Materials and Structures Laboratory & Frontier Collaborative Research Center, Tokyo Institute of Technology, 4259 Nagatsuta, Midori-ku, Yokohama 226-8503, Japan.

(1) Lunsford, J. H. *Catal. Rev.* **1973**, *8*, 135−157.
(2) Che, M.; Tench, A. J. *Adv. Catal.* **1983**, *32*, 1−148.
(3) Bühler, R. E.; Staehelin, J.; Hoigné, H. *J. Phys. Chem.* **1984**, *88*, 2560−2564.
(4) Yanagisawa, T.; Shimizu, T.; Kuroda, K.; Kato, C. *Bull. Chem. Soc. Jpn.* **1990**, *63*, 988−992.
(5) Kresge, C. T.; Leonowicz, M. E.; Roth, W. J.; Vartuli, J. C.; Beck, J. S. *Nature* **1992**, *359*, 710−712.
(6) Bagshaw, S. A.; Prouzet, E.; Pinnavaia, T. J. *Science* **1995**, *269*, 1242−1244.
(7) Radzig, V. A. In *Defects in SiO_2 and Related Dielectrics: Science and Technology*; Pacchioni, G., Skuja, L., Griscom, D. L., Eds.; NATO Science Series; Kluwer Academic Publishers: Dordrecht, Netherlands, 2000; pp 339−370.
(8) Inaki, Y.; Yoshida, H.; Yoshida, T.; Hattori, T. *J. Phys. Chem. B* **2002**, *106*, 9098−9106.
(9) Brower, K. L.; Lenahan, P. M.; Dressendorfer, P. V. *Appl. Phys. Lett.* **1982**, *41*, 251−253.
(10) Griscom, D. L. *J. Non-Cryst. Solids* **1984**, *68*, 301−325.
(11) Miyazaki, T.; Azuma, N.; Fueki, K. *J. Am. Ceram. Soc.* **1984**, *67*, 99−102.
(12) Tsai, T. E.; Griscom, D. L.; Friebele, E. J. *Phys. Rev. B* **1989**, *40*, 6374−6380.
(13) Kajihara, K.; Skuja, L.; Hirano, M.; Hosono, H. *Phys. Rev. Lett.* **2002**, *89*, 135507.
(14) Griscom, D. L.; Stapelbroek, M.; Friebele, E. J. *J. Chem. Phys.* **1983**, *78*, 1638−1651.
(15) Hosono, H.; Abe, Y.; Oyoshi, K.; Tanaka, S. *Phys. Rev. B* **1991**, *43*, 11966−11970.
(16) Griscom, D. L.; Friebele, E. J. *Phys. Rev. B* **1986**, *34*, 7524−7533.
(17) Nishikawa, H.; Nakamura, R.; Ohki, Y.; Nagasawa, K.; Hama, Y. *Phys. Rev. B* **1992**, *46*, 8073−8079.
(18) Shelby, J. E. *J. Appl. Phys.* **1977**, *48*, 3387−3394.

species while excluding the contributions of surface adsorbates. Interstitial O_2 traps mobile H^0 generated by F_2-laser ($\lambda = 157$ nm, $h\nu = 7.9$ eV) photolysis of the SiO−H bonds[13,19,20] to create $HO_2^{\bullet}$,

$$\equiv SiOH \xrightarrow{h\nu=7.9\ eV} \equiv SiO^{\bullet} + H^0 \quad (1)$$

$$O_2 + H^0 \rightarrow HO_2^{\bullet} \quad (2)$$

In this work, we show that the interstitial voids in *a*-SiO_2 play an important role in forming $HO_2^{\bullet}$ in the above mechanism and in stabilizing the resultant $HO_2^{\bullet}$ up to 100 °C.

2. Experimental Section

Commercial synthetic "wet" *a*-SiO_2 pieces containing network-bound SiOH ($\sim 1 \times 10^{20}$ cm^{-3}) and SiCl ($\sim 5 \times 10^{18}$ cm^{-3}) groups, 10 × 4 × 2 mm^3 in size, were used. Heating of the pristine pieces in O_2 ($\sim$3 atm) for 720 h at 900 °C yielded O_2-loaded hydrogenated samples that contain $\sim 10^{17}$ cm^{-3} of interstitial O_2.[21,22] The absorption coefficients of SiOH groups and O_2 at 7.9 eV in this sample were $\sim$35[23] and $\sim$2 cm^{-1},[24,25] respectively. A separate set of pristine pieces was first treated in D_2 ($\sim$3 atm) for 96 h at 900 °C prior to the O_2 loading to obtain O_2-loaded deuterated samples, whose SiOH groups were completely ($\sim$99%) replaced by SiOD groups.[25] The third set of pristine pieces was treated in a vacuum for 240 h at 900 °C to prepare O_2-free hydrogenated samples for use as references for the O_2-loaded samples. The samples were exposed to F_2-laser pulses (LPF-210, Lambda Physik, pulse duration $\sim$20 ns) of $\sim$2−10 mJ cm^{-2} $pulse^{-1}$ either at room temperature or at 77 K. To avoid F_2-laser photolysis of interstitial O_2 into a pair of oxygen atoms (O^0), the irradiation was terminated at a small cumulative fluence ($\leq$1 J cm^{-2}). The laser-induced paramagnetic species were measured by an X-band electron paramagnetic resonance (EPR) spectrometer (Bruker, Model E580) at 77 K.

3. Results

Figure 1a shows the EPR spectra of the O_2-free and O_2-loaded hydrogenated samples exposed to F_2-laser light at room temperature with a cumulative fluence of $\sim$1 J cm^{-2}. The EPR spectrum of the O_2-loaded deuterated sample is shown in Figure 1b. In the O_2-free sample, only a very weak signal assigned to the oxygen dangling bond (nonbridging oxygen hole center, NBOHC, $\equiv SiO^{\bullet}$)[26] was observed. In contrast, signals for the O_2-loaded hydrogenated and deuterated samples were much more intense and complicated. The dominant part of the signals was due to one or several unidentified paramagnetic species (hereafter denoted as "*Z*") overlapping the well-known signals of NBOHC and the peroxy radical (POR, $\equiv SiOO^{\bullet}$).[26,27]

To isolate the signal specific to *Z*, the components of NBOHC ($g_1 = 2.0014$, $g_2 = 2.0103$, and $g_3 \approx 2.08$) and POR ($g_1 = 2.0017$, $g_2 = 2.0073$, and $g_3 = 2.070$), whose spectral shapes were recorded using the techniques shown in refs 13, 20 and 28, 29, respectively, were subtracted. Characteristic signals of NBOHC at $\sim$345−347 mT, and of POR at $\sim$334 mT (the g_3 peak, not shown in Figure 1) and $\sim$345 mT, were used to determine the amplitudes of the subtracted components, which are shown in Figure 1a for the case of the hydrogenated sample. The spectrum obtained by the subtraction is referred to as the "extracted spectrum" (Figure 1, traces C). The positions of the peaks remaining in the extracted spectrum were insensitive to small variations in the amplitudes of the subtracted components.

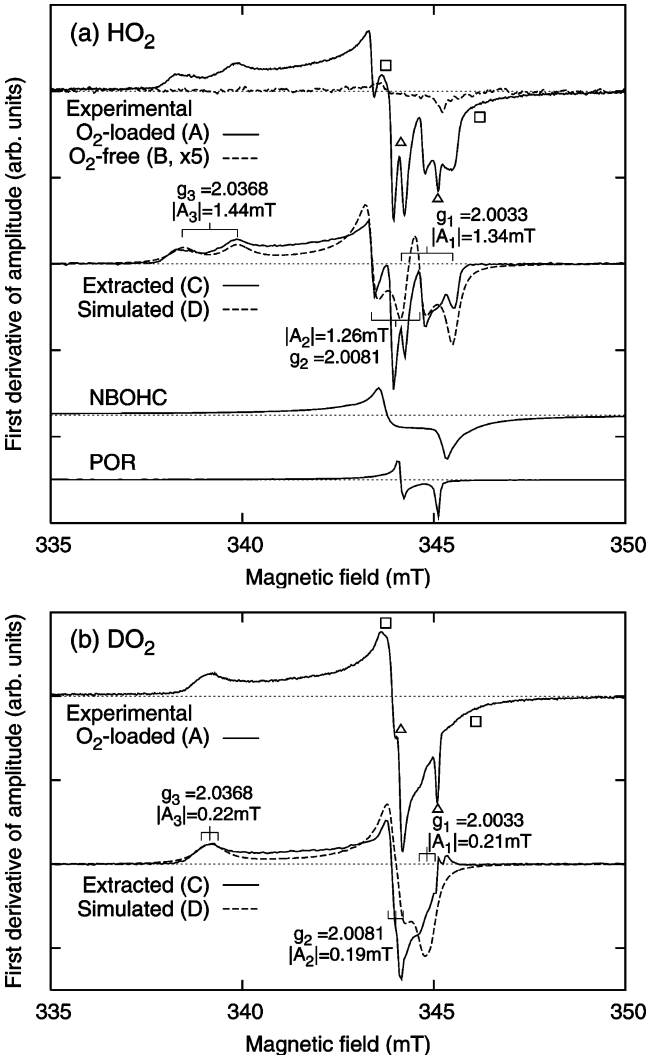

Figure 1. EPR spectra of (a) hydrogenated and (b) deuterated samples exposed to F_2-laser light of $\sim$1 mJ cm^{-2} cumulative fluence at room temperature (recorded at 77 K; microwave power, 20 mW; modulation amplitude, 0.1 mT; modulation frequency, 100 kHz). A new paramagnetic species, also referred to as *Z* in the text, is formed along with NBOHC (□) and POR (△) in the O_2-loaded samples (traces A). In contrast, the only paramagnetic species detected in the O_2-free sample is a small amount of NBOHC (trace B, magnified by 5 times). Subtraction of the NBOHC and POR components from trace A yields the signal due to *Z*, which is assigned to interstitial $HO_2^{\bullet}$ or $DO_2^{\bullet}$ (traces C). For the hydrogenated sample, the subtracted NBOHC and POR components are shown in the lower part of panel (a). A simulated spectrum of the hydrogenated sample [trace D in panel (a)] was calculated using the *g* and *A* values listed in Table 1, and that of the deuterated sample [trace D in panel (b)] was obtained by the same procedure but employing the nuclear parameters of D instead of H.

(19) Kajihara, K.; Skuja, L.; Hirano, M.; Hosono, H. *Appl. Phys. Lett.* **2001**, *79*, 1757−1759.
(20) Hosono, H.; Kajihara, K.; Suzuki, T.; Ikuta, Y.; Skuja, L.; Hirano, M. *Solid State Commun.* **2002**, *122*, 117−120.
(21) Kajihara, K.; Miura, T.; Kamioka, H.; Hirano, M.; Skuja, L.; Hosono, H. *J. Ceram. Soc. Jpn.* **2004**, *112*, 559−562.
(22) Kajihara, K.; Kamioka, H.; Hirano, M.; Miura, T.; Skuja, L.; Hosono, H. *J. Appl. Phys.* **2005**, *98*, 013529.
(23) Kajihara, K.; Hirano, M.; Uramoto, M.; Morimoto, Y.; Skuja, L.; Hosono, H. *J. Appl. Phys.* **2005**, *98*, 013527.
(24) Morimoto, Y.; Nozawa, S.; Hosono, H. *Phys. Rev. B* **1999**, *59*, 4066−4073.
(25) Kajihara, K.; Hirano, M.; Skuja, L.; Hosono, H. *Phys. Rev. B* **2005**, *72*, 214112.
(26) Stapelbroek, M.; Griscom, D. L.; Friebele, E. J.; Sigel, G. H., Jr. *J. Non-Cryst. Solids* **1979**, *32*, 313−326.
(27) Friebele, E. J.; Griscom, D. L.; Stapelbroek, M.; Weeks, R. A. *Phys. Rev. Lett.* **1979**, *42*, 1346−1349.
(28) Kajihara, K.; Skuja, L.; Hirano, M.; Hosono, H. *Phys. Rev. Lett.* **2004**, *92*, 015504.
(29) Kajihara, K.; Skuja, L.; Hirano, M.; Hosono, H. *J. Non-Cryst. Solids* **2004**, *345 & 346*, 219−223.

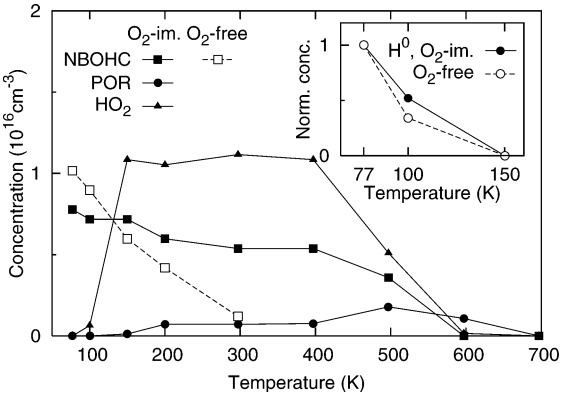

Figure 2. Variations in concentrations of $HO_2^{\bullet}$, NBOHC, POR, and H^0 (inset) in the O_2-free (open symbols) and O_2-loaded (filled symbols) hydrogenated samples with isochronal annealing for 10 min at each temperature. The concentrations of H^0 are normalized to the signal intensity at 77 K because of the difficulty in evaluating the absolute value due to the microwave-saturation effect. The paramagnetic centers were created by exposure to F_2-laser light at 77 K (cumulative fluence, ~0.2 mJ cm^{-2}).

The thermal stability of paramagnetic species was examined by isochronal pulse annealing of the O_2-loaded hydrogenated sample irradiated with F_2-laser light (cumulative fluence, ~0.2 J cm^{-2}) at 77 K, for 10 min up to 673 K (Figure 2). A similar sequence was applied to the O_2-free hydrogenated sample. EPR spectra, recorded at 77 K after each irradiation or annealing step, were deconvoluted following the procedure shown in Figure 1a, to evaluate the concentrations of NBOHC, POR, *Z*, and H^0. The temperature dependences of these are summarized in Figure 2. Because of a distinct microwave saturation effect, the concentration of H^0 (sharp doublets at ~318 and 368 mT) was determined in relative units only, normalized to the initial signal intensity at 77 K.

In both the O_2-free and O_2-loaded samples, the main paramagnetic centers created at 77 K were NBOHC and H^0, and they were progressively annihilated with an increase in the annealing temperature. However, in the O_2-loaded sample, NBOHC disappeared at a much higher temperature (~600 K), and the new signal *Z* appeared along with the decay of H^0. In addition, POR was found to be formed above 200 K, suggesting that interstitial O_2 is partially photolyzed at 77 K, and a part of the resultant O^0 becomes mobile above 200 K, turning NBOHC into POR.[28] Thermal decomposition of paramagnetic species in the O_2-loaded sample started above 400 K and was almost complete at 700 K.

4. Discussion

The shape of the "extracted spectrum" remains the same during the change in the intensity in the isochronal annealing experiment, indicating that the extracted spectrum most likely belongs to a single type of paramagnetic species *Z*. There is strong evidence that *Z* is $HO_2^{\bullet}$ generated via eq 2. First, *Z* is observed only in the O_2-loaded samples. Second, the distinct difference in the extracted spectra between the hydrogenated and deuterated samples indicates the presence of hydrogen atoms that cause a large hyperfine interaction. Third, the formation of *Z* is accompanied by the decay of interstitial H^0. To confirm this supposition, line-shape simulation of the extracted spectra was performed. The mutual orientations of principal axes of $\boldsymbol{g}$ and hyperfine ($\boldsymbol{A}$) tensors listed in Table 1 were set identical to those of $HO_2^{\bullet}$ reported in ref 30. Considering that the paramagnetic species is randomly oriented in *a*-SiO_2, the extracted spectrum of the hydrogenated sample (Figure 1a) was simulated via the least-squares method by optimizing the principal values of $\boldsymbol{g}$, $\boldsymbol{A}$, and the line width tensors, and the Gaussian−Lorentzian ratio of the pseudo-Voigt peak convolution function. The optimized principal values of $\boldsymbol{g}$ and $\boldsymbol{A}$ (Table 1), which were obtained by adopting an almost pure (~95%) Lorentzian convolution function, agree well with those determined for $HO_2^{\bullet}$ trapped in ice[30−34] and inert gas matrixes.[35,36] The resultant parameters were then used to generate the signal of the deuterated species by merely accounting for the differences between H and D (nuclear spin, $I_H = 1/2$, $I_D = 1$; $\boldsymbol{A}_H = 6.5144\ \boldsymbol{A}_D$), resulting in a good agreement between the extracted and simulated spectra (Figure 1b). Thus, we conclude that the unidentified species is interstitial $HO_2^{\bullet}$.

Table 1. Principal Values of $\boldsymbol{g}$ and Hyperfine ($\boldsymbol{A}$) Tensors Determined for $HO_2^{\bullet}$ in *a*-SiO_2[a]

		Direction cosines				Direction cosines		
	g	1	2	3	*A* (mT)	1	2	3
xx	2.0033 ± 0.001	1	0	0	−1.34 ± 0.2	−1	0	0
yy	2.0081 ± 0.001	0	1	0	−1.44 ± 0.2	0	0.105	0.995
zz	2.0368 ± 0.001	0	0	1	−1.26 ± 0.2	0	0.995	−0.105

[a] It was assumed that the *z* axis of $\boldsymbol{A}$ is along the O−H bond and has an angular separation of 96° relative to the *z* axis of $\boldsymbol{g}$, which is in the molecular plane and lies nearly along the O−O bond.[30] The *x* axes of $\boldsymbol{g}$ and $\boldsymbol{A}$ were both taken to be perpendicular to the molecular plane. The signs of the principal values of $\boldsymbol{A}$ were determined following the data of gaseous $HO_2^{\bullet}$, reported in refs 37 and 38.

This assignment was further verified by the magnitudes of the isotropic (a_{iso}) and anisotropic ($\boldsymbol{T}$) parts of $\boldsymbol{A}$,[39] calculated as

$$\boldsymbol{A} = a_{iso}\mathbf{1} + \boldsymbol{T} = -1.35 \times \mathbf{1} + \begin{vmatrix} 0.01 & & \\ & -0.09 & \\ & & 0.09 \end{vmatrix} \quad (3)$$

where **1** is the 3 × 3 unit matrix. a_{iso} has a negative sign, and its absolute value is ~3% of the isotropic hyperfine constant of a free H atom (50.7 mT), but it is larger than the components of the anisotropic part $\boldsymbol{T}$. These results accord well with the characteristic features of $HO_2^{\bullet}$, namely that the unpaired electron is located on the π^* orbital of the O−O bond and that spin polarization is the dominant origin of the hyperfine interaction.[39]

The EPR line width of $HO_2^{\bullet}$ in *a*-SiO_2 is narrower than that in H_2O ice,[30−34] allowing the hyperfine splitting resulting from the H nucleus to be well resolved. This is due to the absence of

(30) Bednarek, J.; Plonka, A. *J. Chem. Soc., Faraday Trans. 1* **1987**, *83*, 3737−3747.
(31) Smith, R. C.; Wyard, S. J. *Nature* **1960**, *186*, 226−228.
(32) Wyard, S. J.; Smith, R. C.; Adrian, F. J. *J. Chem. Phys.* **1968**, *49*, 2780−2783.
(33) Bednarek, J.; Plonka, A.; Hallbrucker, A.; Mayer, E.; Symons, M. C. R. *J. Am. Chem. Soc.* **1996**, *118*, 9387−9390.
(34) Mihelcic, D.; Volz-Thomas, A.; Pätz, H. W.; Kley, D.; Mihelcic, M. *J. Atmos. Chem.* **1990**, *11*, 271−297.
(35) Adrian, F. J.; Cochran, E. L.; Bowers, V. A. *J. Chem. Phys.* **1967**, *47*, 5441−5442.
(36) Norizawa, K.; Hirai, M.; Kanosue, K.; Ikeya, M. *Jpn. J. Appl. Phys.* **2000**, *39*, 6759−6762.
(37) Saito, S. *J. Mol. Spectrosc.* **1977**, *65*, 229−238.
(38) Barnes, C. E.; Brown, J. M.; Carrington, A.; Pinkstone, J.; Sears, T. J.; Thistlethwaite, P. J. *J. Mol. Spectrosc.* **1978**, *72*, 86−101.
(39) Weil, J. A.; Bolton, J. R.; Wertz, J. E. *Electron Paramagnetic Resonance: Elementary Theory and Practical Applications*; John Wiley & Sons: New York, 1994.

superhyperfine interaction between $HO_2^•$ and the surrounding matrix. Analogous spectra with reduced line widths have been observed for $HO_2^•$ in D_2O ice[34] and CO_2.[36]

In "wet" O_2-free *a*-SiO_2 exposed to F_2-laser light, a large amount of NBOHC is transiently formed by efficient (quantum yield > 0.1) cleavage of SiO−H bonds.[13,19,20] The resultant NBOHC quickly decays at room temperature through recombination with the photogenerated mobile H^0 and H_2, leaving only a small amount of persistent NBOHC.[19,13] In contrast, in the O_2-loaded sample, a large part of NBOHC remains unreacted at room temperature (Figures 1 and 2) as a result of the competitive trapping of mobile H^0 by O_2 (eq 2), preventing recombination of H^0 with NBOHC. The trapping is efficient, because the cumulative concentration of H^0 induced at 77 K under a similar irradiation fluence ($\sim 2 \times 10^{16}$ cm^{-3} [13,19]) is roughly equal to the concentration of $HO_2^•$ subsequently formed above 150 K ($\sim 1 \times 10^{16}$ cm^{-3}) in the annealing experiment (Figure 2). A study of the quenching of singlet photoluminescence of O_2 by SiOH groups suggests a homogeneous distribution of O_2 and SiOH groups in O_2-loaded samples of present type.[40] The average separation between O_2 and SiOH groups ($\sim$1 nm) is sufficiently smaller than the average diffusion length of H^0 in *a*-SiO_2 ($\sim$1−100 nm in 1 s at 100 K[12]), supporting the formation of $HO_2^•$ via eq 2.

The formation of $HO_2^•$ through the reaction of O_2 with H^0 has been intensively studied in the gas phase.[41−43] The reaction is very slow when the participation of an inert gas molecule M that takes the excess energy away from the reaction intermediate (triple collision),

$$O_2 + H^0 + M \rightarrow HO_2 + M \quad (4)$$

is absent. However, $HO_2^•$ is efficiently formed in *a*-SiO_2. Thus, it seems likely that the dissipation of the excess energy of the reaction intermediate through its collisions with the *a*-SiO_2 network plays a vital role in the creation of $HO_2^•$ in interstitial voids in *a*-SiO_2. The presence of such energy redistribution processes is well-known for reactions in solid gas matrixes,[44] including the formation of $HO_2^•$.[45,46] However, it is interesting that the same reaction occurs near room temperature in *a*-SiO_2, a covalent macromolecule with a three-dimensional tetrahedral network. The dimerization of H^0 in *a*-SiO_2,[10,12,13] which is another triple collision reaction in the gas phase,[47,48]

$$H^0 + H^0 + M \rightarrow H_2 + M \quad (5)$$

should take place by an analogous mechanism in *a*-SiO_2.

Although the numerical simulation generally reproduced the peak positions of the experimental EPR spectra well, some discrepancies still remain in the spectral shape and the relative peak amplitudes (Figure 1). This is probably due to the thermal motion of paramagnetic species,[2] which makes the simulation using a static spin-Hamiltonian difficult, particularly when the motion is anisotropic.[49] A reason for such anisotropic motion is the steric hindrance. The interstitial voids in *a*-SiO_2 would be too small for $HO_2^•$ to rotate unhindered, considering that O_2, whose size and shape are similar to those of $HO_2^•$, does not rotate freely about the axes perpendicular to the O−O bond in *a*-SiO_2.[50] Another possible factor restricting the free motion of $HO_2^•$ is hydrogen bonding,[32,33,45] which can take place with the bridging oxygen atoms and SiOH groups in the *a*-SiO_2 network. An analogous type of hydrogen bonding is suggested for interstitial H_2O in *a*-SiO_2.[25] It is considered that hydrogen bonding suppresses the motion of $HO_2^•$ in ice,[32,33] whereas its absence allows $HO_2^•$ to rotate in solid Ar even at 4 K.[35] On the basis of these considerations, we suggest a rocking motion[51] of $HO_2^•$ in *a*-SiO_2 at 77 K.

5. Conclusions

The hydroperoxy radical ($HO_2^•$) was synthesized in bulk amorphous SiO_2 (*a*-SiO_2), and its properties were studied by electron paramagnetic resonance (EPR). Interstitial O_2 in *a*-SiO_2 is efficiently converted into $HO_2^•$ through reaction with a mobile hydrogen atom (H^0), which is formed by F_2-laser photolysis of SiOH groups. It is likely that the formation of $HO_2^•$ is promoted by collisions of the reaction intermediate with the *a*-SiO_2 network that dissipates the excess energy of the intermediate. The resultant $HO_2^•$ is stable against thermal annealing up to 100 °C, due to its encapsulation in the chemically inert *a*-SiO_2 network. It was demonstrated that bulk SiO_2 provides nanospaces appropriate for photomanipulation of small reactive compounds.

Acknowledgment. We thank Dr. S. Matsuishi of Tokyo Institute of Technology for useful discussions.

JA0571390

(40) Kajihara, K.; Kamioka, H.; Hirano, M.; Miura, T.; Skuja, L.; Hosono, H. *J. Appl. Phys.* **2005**, *98*, 013528.
(41) Kurylo, M. J. *J. Phys. Chem.* **1972**, *76*, 3518−3526.
(42) Lee, L. C. *J. Chem. Phys.* **1982**, *76*, 4909−4915.
(43) Schwab, J. J.; Brune, W. H.; Anderson, J. G. *J. Phys. Chem.* **1989**, *93*, 1030−1035.
(44) Himmel, H.-J.; Downs, A. J.; Greene, T. M. *Chem. Rev.* **2002**, *102*, 4191−4241.
(45) Nelander, B. *J. Phys. Chem. A* **1997**, *101*, 9092−9096.
(46) Khriachtchev, L.; Pettersson, M.; Lignell, A.; Rasanen, M. *J. Am. Chem. Soc.* **2001**, *123*, 8610−8611.
(47) Larkin, F. S. *Can. J. Chem.* **1968**, *46*, 1005.
(48) Trainor, D. W.; Ham, D. O.; Kaufman, F. *J. Chem. Phys.* **1973**, *58*, 4599−4609.
(49) Budil, D. E.; Lee, S.; Saxena, S.; Freed, J. H. *J. Magn. Reson.* **1996**, *A120*, 155−189.
(50) Skuja, L.; Güttler, B.; Schiel, D.; Silin, A. R. *J. Appl. Phys.* **1998**, *83*, 6106−6110.
(51) Matsuishi, S.; Hayashi, K.; Hirano, M.; Tanaka, I.; Hosono, H. *J. Phys. Chem. B* **2004**, *108*, 18557−18568.